Published in final edited form as:
Acta Biomater. 2011 August ; 7(8): 3036–3041. doi:10.1016/j.actbio.2011.04.016.

Clay-Enriched Silk Biomaterials for Bone Formation

Aneta J. Mieszawska[1], **Jabier Gallego Llamas**[1], **Christopher A. Vaiana**[2,3], **Madhavi P. Kadakia**[3], **Rajesh R. Naik**[2,3], and **David L. Kaplan**[1,*]

[1] Department of Biomedical Engineering, Tufts University, Medford, MA 02155

[2] Materials and Manufacturing Directorate, Air Force Research Laboratory, Wright-Patterson AFB, OH 45433

[3] Department of Biochemistry and Molecular Biology, Wright State University, Dayton, OH 45435

Abstract

The formation of silk protein/clay composite biomaterials for bone tissue formation is described. Silk fibroin serves as an organic scaffolding material offering mechanical stability suitable for bone specific uses. Clay montmorillonite (Cloisite ® Na^+) and sodium silicate are sources of osteoinductive silica-rich inorganic species, analogous to bioactive bioglass-like bone repair biomaterial systems. Different clay particle-silk composite biomaterial films were compared to silk films doped with sodium silicate as controls for support of human bone marrow derived mesenchymal stem cells (hMSCs) in osteogenic culture. The cells adhered and proliferated on the silk/clay composites over two weeks. Quantitative real-time RT-PCR analysis revealed increased transcript levels for alkaline phosphatase (ALP), bone sialoprotein (BSP), and collagen type 1 (Col I) osteogenic markers in the cells cultured on the silk/clay films in comparison to the controls. Early evidence for bone formation based on collagen deposition at the cell-biomaterial interface was also found, with more collagen observed for the silk films with higher contents of clay particles. The data suggest that the silk/clay composite systems may be useful for further study toward bone regenerative needs.

Keywords

silk; clay; montmorillonite; stem cells; osteogenesis

1. INTRODUCTION

Bone regeneration is an active process that recapitulates skeletal development. Bone loss caused by bone diseases or fractures represents a challenge in the field in regenerative medicine, as regeneration depends on several factors including cell-scaffold interactions or the presence of soluble molecules like cytokines, growth factors, hormones, ions, and vitamins to support osteogenic regulatory functions [1–3]. Current trends in bone tissue engineering seek scaffold materials that degrade slowly with rates comparable to new bone

CORRESPONDING AUTHOR: David L. Kaplan, Department of Biomedical Engineering, Tufts University, 4 Colby Street, Medford, MA 02155 USA., Phone: (+1) 617 627 3251, Fax: (+1) 617 627 3231, David.Kaplan@tufts.edu.

tissue formation, as well as stimulatory functions promoting osteogenesis. Biomaterials that fulfill these requirements would aid bone therapies.

Silks are fibrous proteins produced by insects or spiders, and provide structural and protective functions [4]. Silkworm silk from *Bombyx mori* is one of the most characterized silks and consists of the heavy and light chains that form fibers with impressive mechanical strength. Additionally, aqueous processing conditions, biocompatibility, and biodegradability of silk fibroin, along with facile chemical modifications, are attractive features often sought in biomaterials [5,6]. These attributes have led to the incorporation of silk fibroin into biomaterials in the tissue engineering field for a wide range of biomedical applications, including osteogenesis [7].

The presence of predominant hydrophobic regions within silk fibroin with repetitive sequences of GAGAGS, GAGAGY, and GAGAGVGY, is responsible for the formation of crystalline beta-sheet secondary structures that control the mechanical properties of silk. The crystallinity can be induced through chemical or physical treatments and the degree of crystallinity specifies silk degradation rates and stability against aqueous and organic solvents [8–10]. Moreover, silks can be processed into gels, films, fibers or sponges, all suitable for different biomedical applications [11–13]. Thus silk fibroin is a suitable material to use in bone tissue engineering where mechanical strength and slow degradation rate enable the exchange or transition to fully functional tissue over time *in vivo*.

Clay minerals are platelets of layered-silicates with high surface area and high aspect ratios. Montmorillonite (MMT), also known as clay, is one of the most commonly used layered silicates with the general formula of $M_x(Al_{4-x}M_{gx})Si_8O_{20}$ [14] and crystal lattice of octahedral sheets of alumina or magnesium fused between two tetrahedral silica sheets. The crystal layers are about 1 nm thick and up to several microns long and organize into stacks with a separating gap filled with alkaline metals that can be easily exchanged with small molecules [15,16]. The intercalating properties, availability, and relatively low cost make clays attractive materials for various industrial applications like rheological modifiers for paints, inks, and greases or additives in plastic materials for food packaging [17,18]. Chemically-modified organoclays have also been studied as sorbents in water purification system [19,20]. The ease with which clay materials form organic-inorganic hybrids has resulted in the formation and study of polymer nanocomposites. The improved tensile properties and thermal stability, and tuning of optical properties or shear thinning, are examples of the impact of clay on nanocomposite materials [21–25].

The loading capacity of clays into polymers has driven interest in incorporating clays into biological systems as delivery vehicles for drugs and DNA, as well as for tissue engineering [14, 26–30]. Clay particles have been employed as additives in dental adhesives to improve shear bond strength, to tailor tensile/mechanical properties or to impact *in vitro* degradation rates, and as encapsulating components within a polymer matrix to enhance cell growth [31–35]. The use of MMT particles in bone therapies has also been suggested, such as in engineered scaffolds with improved thermal stability and cytocompatibility and increased cellular proliferation rates [36, 37].

In the present study silk/clay films were studied as a composite for bone tissue engineering. The silk films served as the supportive biomaterial while the clay/MMT particles were a source of osteoinductive silica species. The silk/clay system was studied with human mesenhymal stem cells (hMSCs) in osteogenic culture to determine impact on bone outcomes, against silk and silk-sodium silicate (SS) controls.

2. MATERIALS AND METHODS

2.1. Film Preparation

Bombyx mori silk cocoons (Fiberworks, Beavercreek OH) were cut into pieces and then boiled for 30 min in 0.02 M Na_2CO_3 to separate the glue-like sericin proteins from the structural fibroin proteins. The fibroin extract was rinsed with 18.2 M-Ω deionized water 3 times and air dried for 16hr, followed by dissolving in 9.3 M LiBr solution at 60°C for 4 hr. The solution, dialyzed against 18.2 M-Ω deionized water using wet dialysis tubes for 48hrs (6 water changes), was subsequently centrifuged twice at 4,500 × g for 10 min, and the supernatant was collected and stored at 4°C. Prior to use, the silk solution was filtered through a 5.0 μm syringe filter. The final concentration of aqueous silk solution was determined (via dehydration and weighing) to be 8 wt %.

Cloisite® Na+ Nanoclay, a sodium modified montmorillonite (MMT) (Southern Clay Products in Gonzales, TX) is a 2:1 layered smectite composed of 2 tetrahedral layers of silicon sandwiching an octahedral layer of aluminum. A stock suspension of 10 mg/ml MMT in deionized H_2O was autoclaved and stored at room temperature. 100 μl aliquots of MMT were washed 3X with 1 mL deionized H_2O and pelleted at 20,000 × g for 5 min, and the pellet was resuspended in 100 μl of deionized H_2O. Aliquots of 25, 50, and 100 μL washed MMT suspension were added to the silk fibroin solution and manually mixed by pipette, yielding a final volume of 1 mL. To create a film, 100 μl of silk-MMT was dropped onto a glass cover slip and rotated at 500 rpm for 15 sec, then 3000 rpm for 45 sec using a Speedline Technologies P6700 Spin Coater. Films were then immersed in a methanol bath for 30 min to crystallize. The final concentration of MMT in each film is calculated to be 0.32, 0 .65, and 1.4 wt % respectively.

A fresh sodium-silicate solution was prepared by mixing 210 μl sodium-silicate reagent grade (Sigma-Aldrich) and 0.5 g Dowex 50 WX8-100 ion exchange resin (Sigma-Aldrich) (which lowers the pH and subsequently initiates polymerization of sodium silicate) in 1 mL de-ionized H2O for 30 seconds yielding a 28% sodium silicate solution, then filtered under vacuum to detach resin from the solution. 500 μl of the filtered solution was mixed with 100 μl PBS buffer (pH 7.4) and used immediately. Aliquots of 25, 50, and 100 μL of the polymerized sodium-silicate solution were added to the silk fibroin solution and manually mixed by pipette, yielding a final volume of 1 mL. To create a film, the above mentioned protocol was followed. The final concentration of sodium silicate in the silk film is calculated to be 0.575%, 1.15%, and 2.3 % respectively. The films were formed as stated above.

2.2. Human mesenhymal stem cell (hMSC) studies

Cell medium ingredients were purchased from Invitrogen (CA, USA) and Sigma-Aldrich (MO, USA). Bone marrow aspirate from a young healthy donor was obtained from Lonza (Walkersville, MD). Frozen low passage (2 or 3) hMSCs were thawed and suspended in growth medium containing high glucose Dulbecco's modified eagle medium (DMEM) supplemented with 10% fetal bovine serum, 1% antibiotic/antimycotic, 1% non-essential amino acids, and 10 ng basic fibroblast growth factor (bFGF). The cells were plated onto the silk films at a density of 5,000 cells/cm^2 and kept in a humidified incubator at 37°C and 5% CO_2. The cells were cultured in hMSC media until 80% confluency and then the media was changed to osteogenic medium containing high glucose Dulbecco's modified eagle medium (DMEM) supplemented with 10% fetal bovine serum, 1% antibiotic/antimycotic, 1% non-essential amino acids, 100 nM dexamethasone, 10 mM β-glycerolphosphate, and 0.05 mM L-ascorbic acid 2-phosphate. The medium was changed every 3–4 days. Cell growth,

morphology, and immunostaining were monitored using a phase contrast light microscope (Carl Zeiss, Jena, Germany) equipped with a Sony Exwave HAD 3CCD color video camera.

2.3.Cell viability

The metabolic activity of cells after 2 weeks in osteogenic culture was quantified using the alamarBlue® assay (Invitrogen, CA, USA) according to the manufacturer's instructions. Briefly, 1 mL of a solution containing basic medium (DMEM supplemented with 1% antibiotic/antimycotic and 10% FBS) with 10% alamarBlue® solution was added to 3 wells from each type of silk film, silk/clay film or tissue culture plastic (TCP), and incubated for 2 h. AlamarBlue® assay was also performed on each type of surface without cells for background correction. A 100 μL aliquot was then taken from each well, and analyzed for fluorescence with excitation at 560 nm and recording the emission at 590 nm. Background fluorescence from the alamarBlue® solution alone was subtracted, and the sample values from 3 wells of each culture were averaged.

2.4.Gene expression using real–time RT-PCR analysis

After osteogenic culture, the cells from three separate wells of each film type were lysed in 0.35 mL Buffer RLT (Qiagen, CA, USA) containing 10% mercaptoethanol, followed by shredding in a QIAshedder (Qiagen). RNA was isolated from the cells using an RNeasy Mini Kit (Qiagen). From this RNA, cDNA was synthesized using a High Capacity cDNA Reverse Transcription Kit (Applied Biosystems, MA, USA) following the manufacturer's instructions. The cDNA samples were analyzed for expression of collagen type I, alkaline phosphatase, and bone sialoprotein relative to the GAPDH housekeeping gene using Assay-on-Demand Gene Expression kits with TaqMan® Universal PCR Master Mix (Applied Biosystems AoD probes). The data were analyzed using the ABI Prism 7000 Sequence Detection Systems software.

2.5. Sample preparation for SEM study and immunostaining

After 2 weeks of osteogenic culture, the coverslips with silk films were removed and fixed in 5% v/v formaldehyde solution in PBS for 30 minutes. Next, the samples were washed in DI water and dehydrated by 20 min incubation in a series of ethanol solutions in water (10%, 30%, 60%, 80%, 90%, 100% vol/vol). Samples then were dried in air and imaged using field emission scanning electron microscopy (FESEM). Immunostaining of the fixed cells was performed using antisera from rabbit raised against collagen I (ab292: Abcam, MA, USA) at a concentration of 4.5 μg/ml. The staining was revealed using the HISTOSTAIN-SP kit (Invitrogen, CA, USA) that use the Labeled-[strept] Avidin-Biotin method following the manufacturer instructions. Briefly, the cells were incubated with the primary antibody followed by biotinylated secondary antibody. Antibody binding was visualized by streptavidin conjugation and DAB reagent from a kit which will turn brown in the location of the antibody. Finally the cells were counter-stained with a solution of hematoxyline staining the cells blue.

2.6. Statistical analysis

The statistical analysis of the results was performed using a two-sided Student s t-test in Excel with $p<0.05$ significance.

3. RESULTS

3.1. Cell Growth and Viability

Cells seeded on silk/MMT and silk/SS films showed good adhesion and proliferation. No cell detachment from the films was observed during expansion as well as during two weeks

of osteogenic culture. These results were similar for the control samples that included silk films alone and TCP. Five days after seeding cells reached ~90% confluency and were subjected to osteogenic stimuli. During the initial growth phase cells showed spindle-like shapes characteristic of undifferentiated fibroblastic hMSCs (Figure 1), while two days after differentiation into osteogenic lineages cell morphology changed to uniform and closely packed flattened cells that covered the film surface. The cell viability was assessed with alamarBlue® assay performed after 2 weeks of osteogenic culture. The results for cells grown on silk/MMT and silk/SS films were compared with cells grown on control TCP and silk films. There was no statistical difference in cell viability for all samples except for the cells grown on silk/0.65% MMT films, where a slightly lower cell number was found when compared to the controls (Figure 2). These results indicate that the addition of SS or MMT to the silk films supported cell-biomaterial interactions and did not cause significant changes in cell survival on the different biomaterial surfaces.

3.2. Gene expression

Osteogenic gene transcript levels for the cells grown on silk films with SS and high and low MMT (0.32% and 1.4%) content with respect to the control samples (TCP and silk only) were evaluated by real-time qRT-PCR (Figure 3). Up-regulation of collagen type I (Col 1) was found when the cells were cultured on silk films with addition of SS (1.15% and 2.3%) and MMT (0.32% and 1.4%), with respect to the control samples. The expression of bone sialoprotein (BSP) was elevated on silk films that contained 0.32 and 1.4% MMT, whereas the BSP transcript levels on silk films containing SS were comparable to BSP expression on the control samples. Similarly, alkaline phosphatase (ALP) was upregulated only for cells cultured on the MMT-containing silk films.

3.3. The formation of extracellular matrix (ECM)

The silk/MMT and silk/SS biomaterials have the potential to induce cells to produce bone-like extracellular matrices. The formation of extracellular matrix was evaluated by SEM and immunostaining. Figure 4 shows representative SEM images of silk/MMT samples revealing the biomaterial surface after two weeks of osteogenic culture. In Figure 4A, the silk/0.32% MMT film surface was covered with mineral particles. The zoomed in region of the same sample shown in Figure 4B reveals additional material around the particles with a few fibrous structures next to the mineral nodules. Increasing the MMT concentration within silk films to 0.65% resulted in the higher content of mineral nodules on the composite film surface and the amount of fibrous structures surrounding the particles increased (Figure 4C-D). The silk films with 1.4% MMT content and closely dispersed MMT particles led to the formation of fibrous networks interconnected with mineral nodules. The coverage of fibers increased with increasing amounts of MMT within the silk films (Figure 4E-F), and number of fibers over 10 μm^2 area was equal to 10 ± 5 (0.32 MMT), 31 ± 9 (0.64MMT), and 158 ± 19 (1.4% MMT). There was lower ECM production on silk film only and on TCP (Figure 4G-H). The analysis of silk films with SS showed no evidence for ECM on the films surface after two weeks of osteogenic culture. The representative images for low (0.575 %) and high (2.3 %) SS doping are shown in Figure 4, frames I and J, respectively. Immunostaining demonstrated collagen type I deposition on the silk/clay surface. The representative image in Figure 5A of a silk/clay film with 1.4% clay content showed collagen fibers (brown stain) and cells (blue stain). The control negative staining in Figure 5B, performed without primary antibody against collagen, shows only cells stained blue, and indicates that there are no nonspecific interactions of secondary antibody with collagen.

4. DISCUSSION

Enhanced bone formation by silica-rich biomaterials has been established [38]. In the present work, we aimed to study if clay particles provided osteogenic stimulus to hMSCs and enhanced the production of bone-related extracellular matrix. We choose clay particles as an additive to the silk matrix since naturally occurring clay minerals are composed of osteoinductive silica, as well as magnesium required for healthy bone growth. We expected increased cell proliferation, differentiation, and consequently enhanced deposition of ECM components with time in cell culture in response to these inorganic components in the clay. Good cell adhesion to the biomaterial surface directly influences cell morphology and its ability to proliferate and induce differentiation, enhancing viability at the same time [39]. Two days after cells were subjected to osteogenic stimuli the morophology changed from spindle-like shapes characteristic of undifferentiated hMSCs to elongated, flattened cells closely packed on the silk film surfaces. Moreover after 2 weeks in osteogenic culture cells adhered well to the biomaterial surface and no cell detachment was observed during culture.

Although clay particles are widely used in industrial applications there are a limited number of reports that investigate their toxicological effects upon exposure. High doses (~20%) of organo-modified montmorillonite within a polymer matrix significantly reduced cellular proliferation [35]. This impact can originate from poor solubility of organo-clay particles as it was shown that particles with limited solubility can lead to inflammation and release of reactive oxygen species (ROS) causing genotoxicity [40,41]. The reports on generation of ROS by natural montmorillonite (Cloisite ® Na^+) appear to differ [42,43] and more research seems to be necessary to establish the sources of potential toxicity. In our studies, we observed high viability of hMSCs grown on silk/clay (Cloisite ® Na^+) surface with the lowest (0.32 %) load of mineral particles within the silk film after 14 days of osteogenic culture. The cell viability on silk/clay 0.32 % films was comparable to the viability observed on control samples that did not contain any additives like silk film only and TCP. The viability considerably decreased with higher doses of clay particles within silk film. The presence of 0.64 % and 1.4 % of clay particles may lead to higher concentration of ionic moieties within cell vicinity leading to slightly lower viability performance. This data suggests that there might be a threshold value for clay particles load and additional increasing the amount of clay within silk film could be a source of potential toxicity.

We also evaluated the effects of the silk/clay biomaterials on osteogenic transcript levels since the silica dissolution ions have been shown to increase the expression of osteogenic markers [40,44]. The enhanced behavior of osteoblasts subjected to ions derived from bioactive glass occurs at the gene, protein, and extracellular matrix levels [45]. We expect slow dissolution of silica-rich clay particles embedded in silk matrix with prolonged time in culture. The presence of silica ions in the culture media was confirmed by inductively coupled plasma (ICP) analysis after one week of osteogenic culture, and cumulative silica ions concentration for all silk/MMT films was in the range between 1.75 and 1.88 ppm. The ICP results confirmed dissolution of clay particles, and the presence of silica ions suggests that also other constitutive clay ions might be present in the culture media and influence the cell behavior. The results of qRT-PCR for the expression of bone specific genes after 2 weeks of osteogenic culture showed statistically significant upregulation of alkaline phosphatase (ALP), bone sialoprotein (BSP), and collagen type 1 (Col 1) for cells cultured on the silk/clay films from lowest (0.32%) to highest (1.4%) clay particle content when compared to gene expression levels on silk film only and TCP control samples. Also, slight upregulation of Col 1 was observed for cells grown on silk/sodium silicate films when compared to cells grown on TCP. These findings demonstrate that silk/clay films have osteoinductive properties which directly affect osteogenesis through the enhancement of the

expression of bone specific markers. Also, clays are rich in other mineral ions that if released during particle dissolution could further enhance the osteoblast performance.

The elevated levels of collagen transcript suggest early formation of collagen on the biomaterial surface. The direct relationship between enhanced collagen type 1 gene expression and increased formation of extracellular matrix has been previously shown [45]. Bone formation by the hMSCs subjected to osteogenic stimulation follows ECM deposition in an irregular pattern that subsequently arranges into lamellar structures [46]. Also, minerals rich in silica promote collagen-fibril self assembly aiding in formation of collagen fibril “nuclei” [47,48]. The SEM images of the cell-surface interface of silk/clay films revealed fibrillar structures associated with the mineral nodules. More importantly, a higher density of fibrils was observed on surfaces with increased content of clay particles within silk films. Interestingly, no fibrillar structures were observed on silk films doped with SS which may suggest that the presence of mineral particles within silk film is a necessary element to promote fibrils self assembly. We validated the samples for collagen by immunostaining. These stains confirm that the fibrillar structures originate form collagen and are consistent with the qRT-PCR results for collagen gene expression which indicate the deposition of collagen-related ECM. These observations show the enhanced effect that silk/clay biomaterials have on collagen synthesis.

5. CONCLUSIONS

Silk/clay biomaterial composites supported bone-related outcomes in the present study, suggesting further studies toward bone related applications as composite biomaterials. The biomaterials supported the attachment, proliferation, and osteogenic differentiation of hMSCs, maintaining high cell viability. The hMSCs were able to produce the ECM with concurrent upregulation of osteogenic markers as evidenced by immunostaining and RT-PCR. The silk/clay system possesses osteoinductive properties and may be interesting candidate for bone tissue engineering.

Acknowledgments

This work was performed in part at the Center for Nanoscale Systems (CNS), a member of the National nanotechnology Infrastructure Network (NNIN) at Harvard University, which is supported by the national Science Foundation under NSF award no. ECS-0335765. The authors thank the NIH (DE017207, EB003210, EB002520) for support of the research.

References

1. Kokubo T, Kim HM, Kawashita M. Novel bioactive materials with different mechanical properties. Biomaterials. 2003; 24:2161–2175. [PubMed: 12699652]
2. Ter Brugge PJ, Jansen JA. In vitro osteogenic differentiation of rat bone marrow cells subcultured with and without dexamethasone. Tissue Eng. 2002; 8:321–331. [PubMed: 12031120]
3. Sakiyama-Elbert SE, Hubbell JA. Functional biomaterials: design of novel biomaterials. Annu Rev Mater Res. 2001; 31:183–201.
4. Omenetto FG, Kaplan DL. New opportunities for an ancient material. Science. 2010; 329:528–531. [PubMed: 20671180]
5. Lovett M, Cannizzaro C, Daheron L, Messmer B, Vunjak-Novakovic G, Kaplan DL. Silk fibroin microtubes for blood vessel engineering. Biomaterials. 2007; 28:5271–5279. [PubMed: 17727944]
6. Minoura N, Tsukada M, Nagura M. Physico-chemical properties of silk fibroin membrane as a biomaterial. Biomaterials. 1990; 11:430–434. [PubMed: 2207234]
7. Leal-Egaña A, Scheibel T. Silk-based materials for biomedical applications. Biotechnol Appl Biochem. 2010; 55:155–167. [PubMed: 20222871]

8. Jin H-J, Park J, Karageorgiou V, Kim U-J, Valluzzi R, Cebe P, Kaplan DL. Water-Stable Silk Films with Reduced β-Sheet Content. Adv Funct Mater. 2005; 15:1241–1247.
9. Winkler S, Wilson D, Kaplan DL. Controlling beta-sheet assembly in genetically engineered silk by enzymatic phosphorylation/dephosphorylation. Biochemistry. 2000; 39:12739–12746. [PubMed: 11027155]
10. Drummy LF, Farmer BL, Naik RR. Correlation of the β-sheet crystal size in silk fibers with the protein amino acid sequence. Soft Matter. 2007; 3:877–882.
11. Tamada Y. New process to form a silk fibroin porous 3-D structure. Biomacromolecules. 2005; 6:3100–3106. [PubMed: 16283733]
12. Jin HJ, Fridrikh SV, Rutledge GC, Kaplan DL. Electrospinning Bombyx mori silk with poly(ethylene oxide). Biomacromolecules. 2002; 3:1233–1239. [PubMed: 12425660]
13. Kim UJ, Park J, Li C, Jin HJ, Valluzzi R, Kaplan DL. Structure and properties of silk hydrogels. Biomacromolecules. 2004; 5:786–792. [PubMed: 15132662]
14. Park JK, Choy YB, Oh J-M, Kim JY, Hwang S-J, Choy J-H. Controlled release of donepezil intercalated in smectite clays. International Journal of Pharmaceutics. 2008; 359:198–204. [PubMed: 18502063]
15. Alexandre M, Dubois P. Polymer-layered silicate nanocomposites: preparation, properties and uses of a new class of materials. Mat Sci and Eng. 2000; 28:1–63.
16. Katti KS, Katti DR. Relationship of swelling and swelling pressure on silica-water interactions in montmorillonite. Langmuir. 2006; 22:532–537. [PubMed: 16401099]
17. Patel HA, Somani RS, Bajaj HC, Jasra RV. Nanoclays for polymer nanocomposites, paints, inks, greases and cosmetics formulations, drug delivery vehicle and waste water treatment. Bull Mater Sci. 2006; 29:133–145.
18. Pereira de Abreu DA, Paseiro Losada P, Angulo I, Cruz JM. Development of new polyolefin films with nanoclays for application in food packaging. European Polymer Journal. 2007; 43:2229–2243.
19. Wiles MC, Huebner HJ, McDonald TJ, Donnelly KC, Phillips TD. Matrix-immobilized organoclay for the sorption of polycyclic aromatic hydrocarbons and pentachlorophenol from groundwater. Chemosphere. 2005; 59:1455–1464. [PubMed: 15876388]
20. Say R, Birlik E, Erdemgil Z, Denizli A, Ersoz A. Removal of mercury species with dithiocarbamate-anchored polymer/organosmectite compos tes. Journal of Hazardous Materials. 2008; 150:560–564. [PubMed: 17560027]
21. LeBaron PC, Wang Z, Pinnavaia TJ. Polymer-layered silicate nanocomposites: an overview. Applied Clay Science. 1999; 15:11–29.
22. Giannelis EP. Polymer-layered silicate nanocomposites: Synthesis, properties and applications. Applied Organometallic Chemistry. 1998; 12:675–680.
23. Wu Z, Zhou C, Qi R, Zhang H. Synthesis and characterization of nylon l0l2/clay nanocomposites. J Appl Pol Sci. 2002; 83:2403–2410.
24. Katti DR, Ghosh P, Schmidt S, Katti KS. Mechanical properties of sodium montmorillonite interlayer intercalated with amino acids. Biomacromolecules. 2005; 6:3276–3282. [PubMed: 16283756]
25. Sikdar D, Katti DR, Katti KS, Bhowmik R. Insight into molecular interactions between constituents in polymer clay nanocomposites. Polymer. 2006; 47:5196–5205.
26. Liu K-H, Liu T-Y, Chen S-Y, Liu D-M. Drug release behavior of chitosan-montmorillonite nanocomposite hydrogels following electrostimulation. Acta Biomaterialia. 2008; 4:1038–1045. [PubMed: 18337198]
27. Campbell K, Craig DQM, McNally T. Poly(ethylene glycol) layered silicate nanocomposites for retarded drug release prepared by hot-melt extrusion. International Journal of Pharmaceutics. 2008; 363:126–131. [PubMed: 18657600]
28. Lin FH, Chen CH, Cheng WTK, Kuo TF. Modified montmorillonite as vector for gene delivery. Biomaterials. 2006; 27:3333–3338. [PubMed: 16488006]
29. Depan D, Kumar AP, Singh RP. Cell proliferation and controlled drug release studies of nanohybrids based on chitosan-g-lactic acid and montmorillonite. Acta Biomaterialia. 2009; 5:93–100. [PubMed: 18796355]

30. Katti KS, Ambre AH, Peterka N, Katti DR. Use of unnatural amino acids for design of novel organomodified clays as components of nanocomposite biomaterials. Phil Trans R Soc A. 2010; 368:1963–1980. [PubMed: 20308111]
31. Atai M, Solhi L, Nodehi A, Mirabedini SM, Kasraei S, Akbari K, Babanzadeh S. PMMA-grafted nanoclay as novel filler for dental adhesives. Dental Materials. 2009; 25:339–347. [PubMed: 18829096]
32. Lin KF, Hsu CY, Huang TS, Chiu WY, Lee YH, Young TH. A novel method to prepare chitosan/montmorillonite nanocomposites. J Appl Pol Sci. 2005; 98:2042–2047.
33. Zhuang H, Zheng JP, Gao H, Yao KD. *In vitro* biodegradation and biocompatibility of gelatin/montmorillonite-chitosan intercalated nanocomposite. J Mater Sci Mater Med. 2007; 18:951–957. [PubMed: 17221313]
34. Styan KE, Martin DJ, Poole-Warren LA. In vitro fibroblast response to polyurethane organosilicate nanocomposites. J Biomed Mater Res Part A. 2007; 86A(3):571–582.
35. Lewkowitz-Shpuntoff HM, Wen MC, Singh A, Brenner N, Gambino R, Pernodet N, Isseroff R, Rafailovich M, Solkolov J. The effect of organo clay and adsorbed FeO(3) nanoparticles on cells cultured on Ethylene Vinyl Acetate substrates and fibers. Biomaterials. 2009; 30:8–18. [PubMed: 18838163]
36. Katti KS, Katti DR, Dash R. Synthesis and characterization of a novel chitosan/montmorillonite/hydroxyapatite nanocomposite for bone tissue engineering. Biomed Mater. 2008; 3:1–12.
37. Haroun AA, Gamal-Eldeen A, Harding DRK. Preparation, characterization and in vitro biological study of biomimetic three-dimensional gelatin–montmorillonite/cellulose scaffold for tissue engineering. J Mater Sci:Mater Med. 2009; 20:2527–2540. [PubMed: 19629650]
38. Mieszawska AJ, Fourligas N, Georgakoudi I, Ouhib NM, Belton DJ, Perry CC, Kaplan DL. Osteoinductive silk-silica composite biomaterials for bone regeneration. Biomaterials. 2010; 31:8902–8910. [PubMed: 20817293]
39. Chen CS, Mrksich M, Huang S, Whitesides GM, Ingber DE. Micropatterned surfaces for control of cell shape, position, and function. Biotechnol Prog. 1998; 14:356–363. [PubMed: 9622515]
40. Bombonato-Prado KF, Bellesini LS, Junta CM, Marques MM, Passos GA, Rosa AL. Microarray-based gene expression analysis of human osteoblasts in response to different biomaterials. J Biomed Mater Res A. 2009; 88:401–408. [PubMed: 18306281]
41. Schins RP, Knaapen AM. Genotoxicity of poorly soluble particles. Inhal Toxicol. 2007; 19 (Suppl 1):189–198. [PubMed: 17886067]
42. Sharma AK, Schmidt B, Frandsen H, Jacobsen NR, Larsen EH, Binderup ML. Genotoxicity of unmodified and organo-modified montmorillonite. Mutat Res. 2010; 700:18–25. [PubMed: 20433941]
43. Lordan S, Kennedy JE, Higginbotham CL. Cytotoxic effects induced by unmodified and organically modified nanoclays in the human hepatic HepG2 cell line. J Appl Toxicol. 2011; 31:27–35. [PubMed: 20677180]
44. Christodoulou I, Buttery LD, Tai G, Hench LL, Polak JM. Characterization of human fetal osteoblasts by microarray analysis following stimulation with 58S bioactive gel-glass ionic dissolution products. J Biomed Mater Res B. 2006; 77:431–436.
45. Varanasi VG, Saiz E, Loomer PM, Anechta B, Uritani N, Ho SP, Tomsia AP, Marshall SJ, Marshall GW. Enhanced osteocalcin expression by osteoblast-like cells (MC3T3-E1) exposed to bioactive coating glass (SiO_2-CaO-P_2O_5-MgO-K_2O-Na_2O system) ions. Acta Biomater. 2009; 5:3536–3547. [PubMed: 19497391]
46. Shapiro F. Bone development and its relation to fracture repair. The role of mesenchymal osteoblasts and surface osteoblasts. Eur Cell Mater. 2008; 15:53–76. [PubMed: 18382990]
47. Eglin D, Coradin T, Giraud Guille MM, Helary C. Livage Collagen-silica hybrid materials: sodium silicate and sodium chloride effects on type I collagen fibrillogenesis. J Biomed Mater Eng. 2005; 15:43–50.
48. Eglin D, Shafran KL, Livage J, Coradin T, Perry CC. Comparative study of the influence of several silica precursors on collagen self-assembly and of collagen on Si speciation and condensation. J Mater Chem. 2006; 16:4220–4230.

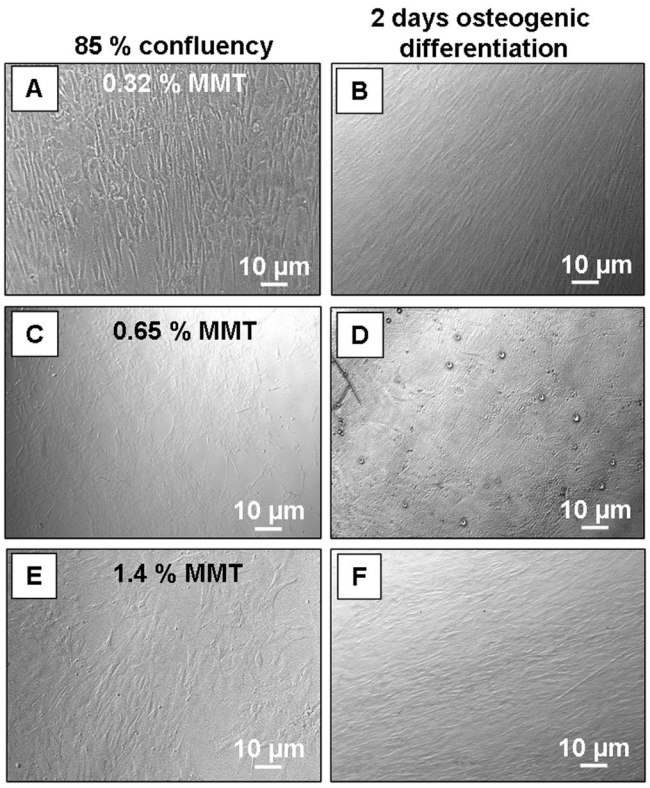

Figure 1.

Optical microscopy images of hMSCs cells grown on silk/clay films before and after osteogenic differentiation. Frames A-B represent 0.32% silk/MMT films, frames C-D are 0.65% silk/MMT films, and frames E-F show 1.4% MMT films. Frames A,C,E = predifferentiation, frames B,D,F are 2 days after osteogenic differentiation.

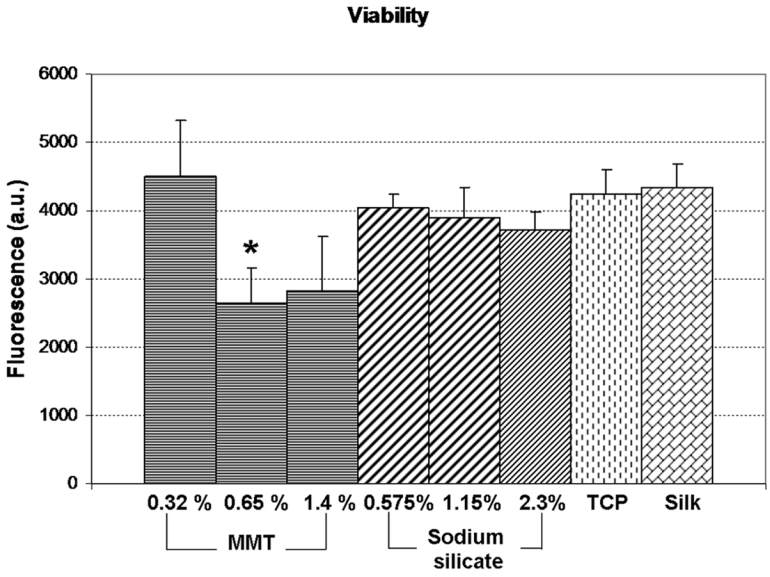

Figure 2.

Alamar blue metabolic activity assay for cells in medium after 2 weeks of osteogenic culture. Each column represents the mean and standard deviation of N=3 independent cultures, and corrected for the background fluorescence of the dye alone. $P<0.05$.

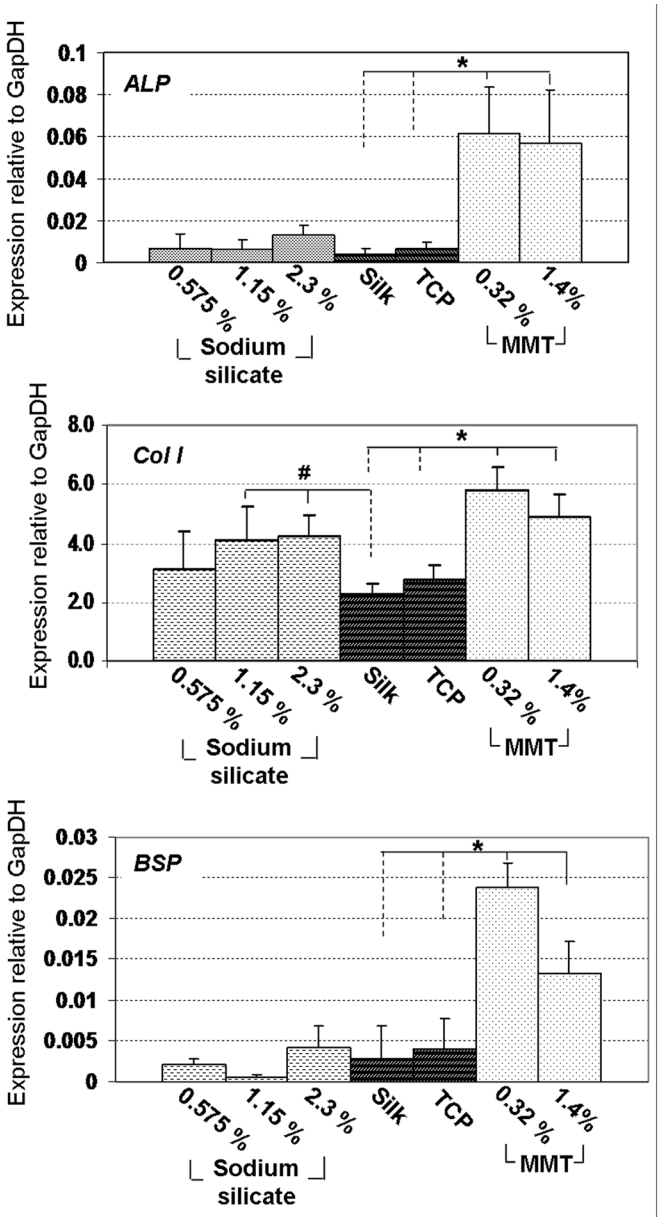

Figure 3.

Osteogenic gene transcript profiles for cells after 2 weeks in osteogenic culture. Each column represents the mean and standard deviation of N = 3 independent cultures. $P < 0.05$.

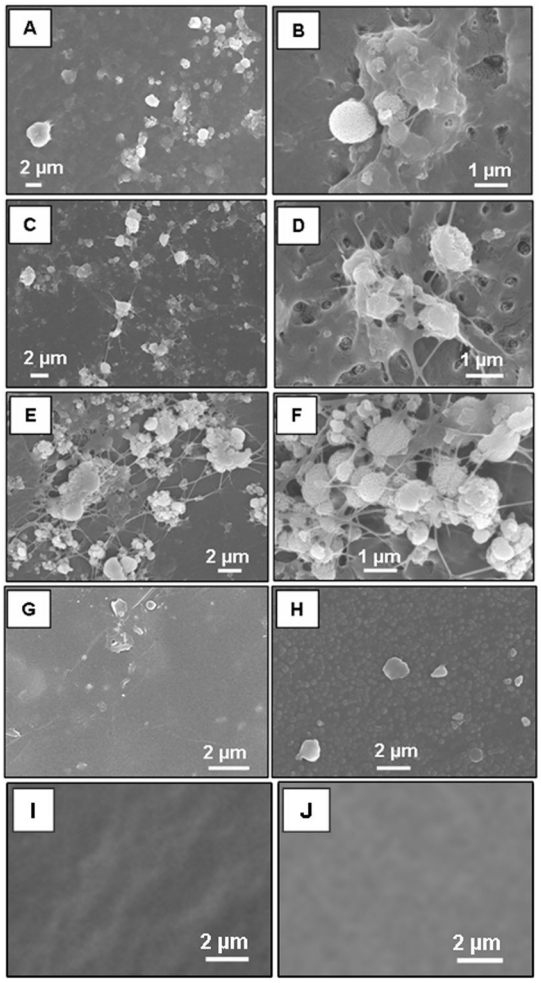

Figure 4.
SEM images of (A-B) silk/ MMT 0.32%, (C-D) silk/MMT 0.65%, (E-F) silk/MMT 1.4%, (G) silk only, (H) TCP, (I) SS 0.575 %, and (J) SS 2.3 % samples after 2 weeks of osteogenic culture.

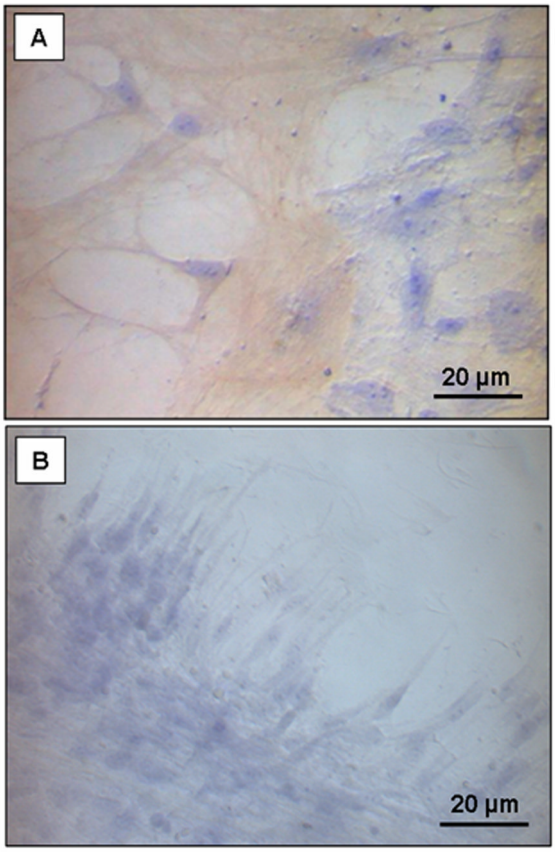

Figure 5.
Optical microscopy images of immunocytochemistry of collagen (frame A). Collagen fibers are stained brown while the cells are stained blue. Frame B represents the negative control (no primary antibody). Immunostaining was performed after 2 weeks of osteogenic culture on silk/ 1.4 % clay film.